Optical and Magnetometric Data Integration for Landmine Detection with UAV

SERGEY A. STANKEVICH, IEVGEN Y. SAPRYKIN
Scientific Centre for Aerospace Research of the Earth,
National Academy of Sciences of Ukraine,
55-B Oles Gonchar str., Kyiv, 01054,
UKRAINE

Abstract: – The joint processing of optical imagery and signals from an onboard fluxgate magnetometer for landmine detection is described in this paper. The basic sensors carried by unmanned aerial vehicles (UAV) enable remote landmine detection, improving the safety of demining. The general methodology for processing both optical and magnetometric data is described. Modern machine learning (ML) and deep learning (DL) techniques are engaged for landmine detection; in particular, optical images are analyzed by a convolutional neural network (CNN), while statistical anomalies are extracted from magnetometer signals. Data integration is performed at the optical and magnetometric detection results level using the Bayesian probabilistic rule. The combination of an optical camera and a magnetometer provides significant reliability enhancement in unburied landmine detection. The proposed methodology will be quite useful for the humanitarian demining of a wide area, improving the reliability of data obtained by remote sensing methods, thus accelerating wide area exploration.

Key-Words: – landmine detection, unmanned aerial vehicle (UAV), optical image, fluxgate magnetometer, magnetometric data, data integration, probability fusion, deep learning, anomaly detection.

Received: August 13, 2024. Revised: December 13, 2024. Accepted: December 27, 2024. Published: December 31, 2024.

1 Introduction

Currently, the problem of humanitarian demining is emerging acutely all over the world, but in Ukraine, it has acquired a terrifying scale. Traditional methods for landmine detection remain dangerous and insufficiently performant when applied to a wide area.

Nowadays, innovative remote detection of explosive devices with UAVs is actively developing worldwide. On the other hand, the presently known methods for remote detection of landmines and other explosive objects using UAVs are not sufficiently reliable. Unfortunately, it must be conceded that there is no universal method for landmine detection with UAVs that would provide acceptable reliability. Nevertheless, the rapid development of optical and signal sensors, as well as data analysis methods, offers hope for the emergence of remote systems that will effectively meet the requirements of humanitarian demining in the foreseeable future. In the meantime, an acceptable solution to this problem may be to integrate the results of optical and magnetometric surveys with UAVs.

The objective of this research is to develop a formalized model for integrating optical and magnetometric data in landmine detection using UAVs.

2 State of the Art

Landmine visual detection in color and infrared images acquired from UAVs remains an important tool for humanitarian demining. Multi- or hyperspectral centimeter-resolution imaging in the optical bands allows for the detection of identifying features of hidden objects' presence, such as dry grass among intact vegetation. Landmine detection based on temperature differences with the surrounding ground is widely used. Such differences can be extracted from images of mid-wave infrared (MWIR, 3-5 μm) or long-wave infrared (LWIR, 7-14 μm).

The scientific fundamentals of computer-aided landmine detection in optical images involve modern methods for pattern recognition using reference features or anomaly detection, [1]. The goal is typically to assess the probability of a landmine's presence at a specific point in the image

based on the multidimensional optical signal features from the corresponding area in the image that matches the size of the landmine, [2]. Landmines and other explosive objects on the land surface exhibit various identifying features, including specific spectral signatures [3], which can be detected in ultra-high spatial resolution optical images acquired from UAVs.

Centimeter-resolution infrared imagery makes it possible to confidently detect landmines and unexploded ordnance by thermal contrast, [4]. Good detection accuracy is provided by specially trained artificial neural networks, [5].

Analysis of existing experience shows that in recent years, the involvement of unmanned aerial vehicles (UAVs) with lightweight non-optical sensors, such as magnetometers, metal detectors, and ground-penetrating radars (GPRs), can significantly increase the performance of landmine detection, [6]. The advantages include the ability to perform precision autonomous flight, multiple sensor installations, high productivity, significant cost reduction, and, most importantly, operator safety, [7]. A series of experiments have demonstrated a fairly high level of landmines and other explosive object detection using a UAV platform equipped with a magnetometer, [8].

GPR is one of the most efficient sensors for buried landmine detection. Modern GPRs are able to identify landmines by analyzing various patterns in the reflected radar signal, [9].

The combination of methods with different physical natures enhances the efficiency and reliability of detecting target objects, [10]. To fuse sensors of different physical natures for landmine detection, various methods can be applied, such as the Bayesian approach, Dempster-Shafer theory, rule-based fusion, voting, fuzzy logic, Kalman filter, and others, [11].

3 Methodology

The general approach to landmine detection with UAVs involves mapping the study area separately with optical and magnetometric drones and then integrating the results obtained. Additionally, sensors of different physical natures are typically installed on different drones and require different flight and surveying modes. This approach does not require internal modification of landmine detection algorithms by various sensors, as a common data representation model ensures matching. In this study, the model used is a probabilistic map of the study area, partitioned according to a probability threshold into detected landmines and an empty background. The probability output is supported by multiple detection algorithms. The integration of data obtained by different methods is also carried out within the framework of a unified probabilistic model, such as a Bayesian one, [12].

3.1 Optical Detection

Landmine detection in optical images is carried out using both traditional machine learning (ML) and deep learning (DL) methods. A pre-trained convolutional neural network (CNN) of YOLO [13] architecture, especially its version Ultralytics YOLOv8 [14], is used for landmine detection in visible imagery (Figure 1), [15], [16], [17], [18], [19], while statistical anomaly extraction within the circular scanning window is utilized for landmine detection in thermal imagery (Figure 2).

Fig. 1: Detected uncovered landmines in the optical image by CNN

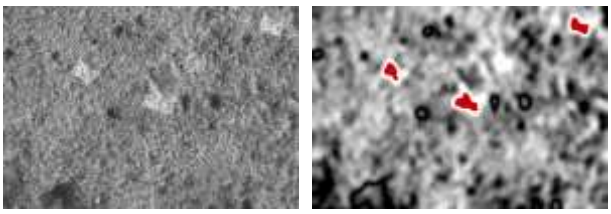

a *b*

Fig. 2: Detected buried landmines in thermal image: *a* – input LWIR image, *b* – probability distribution with threshold masks

Knowing the required resolution of optical imaging from a UAV, it is possible to plan a drone flight mission for mapping an assigned area.

3.2 Magnetometric Detection

A magnetometer is a trace instrument, but it is possible to project the zone of its sensitivity (where a landmine can be detected) into the land surface. The magnetometer's sensitivity zone radius r (see Figure 3) will be determined by the landmine's magnetic field magnitude M, the background magnetic noise μ, and the law of the magnetometer's signal decreasing with a distance $S(r)$, [20], [21], [22], [23].

In response to a quadratically decreasing of the magnetometer's signal with a distance of $S(r) = \frac{G \cdot M}{h^2 + r^2}$, where h is the imaging altitude, G is the proportionality factor, the magnetometer's sensitivity zone radius will be

$$r = h \cdot \sqrt{\frac{M}{\mu \cdot \psi} - 1} \quad (1)$$

where ψ is the signal-to-noise ratio value required for reliable detection.

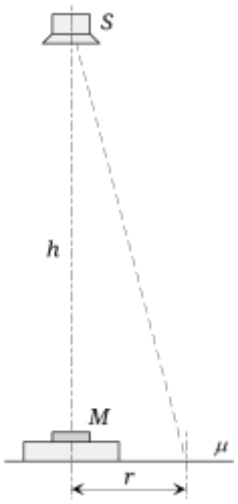

Fig. 3: On the determination of the magnetometer's sensitivity zone radius

Having the magnetometer's sensitivity zone radius, it is possible to determine the flight parameters of the magnetometric drone for continuous coverage of the entire study area with magnetometer footprints, [24], [25], [26], [27]. Inside each footprint, it is possible to calculate the probability of a landmine occurrence by anomaly statistical detection when the magnetometer signal exceeds the background, [28].

3.3 Integration

The integration of the two maps obtained for landmine detection probability – as the results of optical p_o and magnetic p_m surveys – can be performed quite easily. Spatial integration consists of the union/intersection of spatial segments that exceed a predefined probability threshold. Within the intersection segment, the Bayesian probability summation [29] is utilized:

$$p_\Sigma \cong \frac{p_o \cdot p_m}{p_o \cdot p_m + (1 - p_o) \cdot (1 - p_m)} \quad (2)$$

Here, p_Σ is the resultant probability.

Within the non-overlapping extents of segments, the probability remains preserved (Figure 4).

As a result of optical and magnetometric data integration, a single joint map of the landmine detection probability is derived.

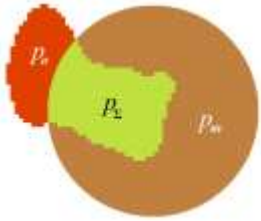

Fig. 4: Probabilities summation within overlapping segments

4 Demonstration

In this section, some illustrations are provided for two major types of landmines – antitank and antipersonnel - and both contain enough magnetic metal to make magnetometer detection reasonable.

4.1 Antitank Mines

The most anticipated candidate for fused optical and magnetic detection is the antitank landmine, which was represented in our research with various types of TM series: TM-62M, TM-62P, and TM-72.

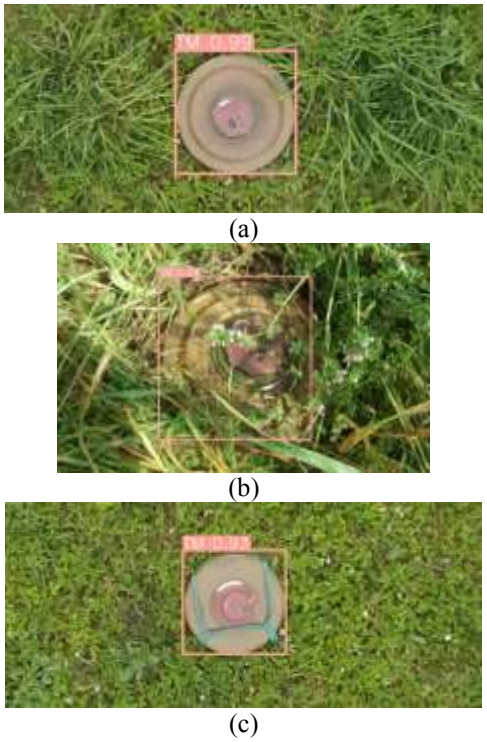

(a)

(b)

(c)

Fig. 5: Antitank landmines of TM-62 series: a) TM-62M perfectly detected by YOLO on the test site; b) TM-62M hidden in vegetation in the field; c) TM-62P3 (plastic casing) detected on the test site

There is a growing trend in the use of robotic platforms for the installation of this type of mine. Therefore, the probability of installation on the surface remains high, making both optical and magnetic detection methods relevant. One of the challenges is the presence of similar antitank plastic mines of the TM 62P series, while another challenge is the appearance of fake mines made from the cheapest materials.

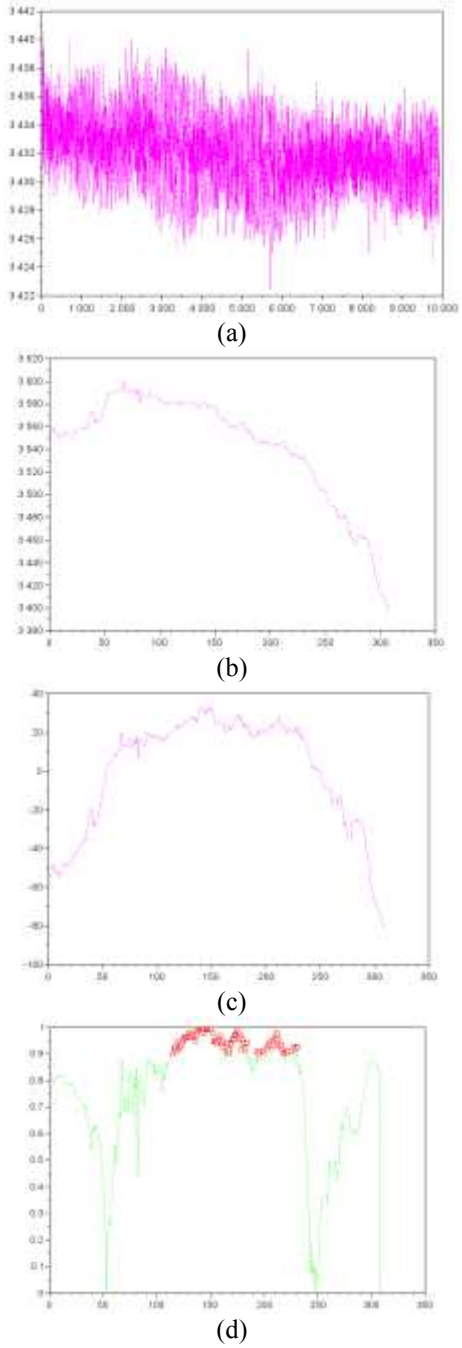

Fig. 6: Steps of processing magnetometric data for TM-62M
a) raw data; b) noise removed, trend from external influence present; c) trend removed; d) probability (threshold 0.9)

Currently, no tools represent the results of magnetic detection "out of the box" in such a user-friendly way as modern computer vision tools based on RGB imagery do. Magnetometric data is subject to processing and requires some operator skills.

Let's consider the case of Figure 5(a) – ideal conditions of the test site, where the optical detection shows a confidence of 99% (for the sake of simplicity, we will treat confidence returned by CNN and probability as synonyms), and magnetic detection shows near 95% (Figure 6(d)). So, according to formula (2), the resulting probability is close to 1, which is just what is expected in ideal conditions.

$$p_{\Sigma} \cong \frac{0.99 \cdot 0.95}{0.99 \cdot 0.95 + (1-0.99) \cdot (1-0.95)} \cong 0.999$$

For a more complex scenario like Figure 4(b), where the mine is partially hidden and optical detection indicates very low confidence, we will assume that magnetic detection yields the same result as it did on the test site – 95%. The calculation will be as follows:

$$p_{\Sigma} \cong \frac{0.04 \cdot 0.95}{0.04 \cdot 0.95 + (1-0.04) \cdot (1-0.95)} \cong 0.44$$

In such cases, we need to keep the threshold low, which may increase the false alarm rate. However, the fusion of probabilities still makes sense.

Finally, let's consider the case of a plastic mine. Magnetic detection gives zero probability, so probability fusion makes no sense. The same situation is observed in the case of a buried TM-62M landmine. Optical detection gives zero confidence, while magnetic detection can still be more than 90% accurate. In such a case, optical detection can be done using indirect signs, but it is reasonable to use a CNN trained on a different dataset, or even some other method of image analysis based on anomaly detection, so the total configuration of the research will be different.

4.2 Antipersonnel Landmines

Another type of landmine, the antipersonnel MON100, optical detection on Figure 7, magnetic detection on Figure 8, is even more illustrative for the fusion method of detection because this type of antipersonnel mine is installed manually and, in most cases, concealed. Therefore, perfect optical detection is less likely than for the TM series. Additionally, due to its shape, more training data is

required to provide appropriate detection by CNN. The MON100 exhibits variability in forms in photos, so more data is needed for the training dataset.

Fig. 7: Antipersonnel MON100 detection: mistakenly detected as TM mine because of its round shape and mistakenly detected as very similar MON200

Currently, the detection of MON100 and MON200 is less confident than that of the TM series. Combining MON100 and similar MON200 into a single class may be reasonable. Using the MON series as an example, we can demonstrate that the optimal dataset structure for optical landmine detection is still the subject of active research.

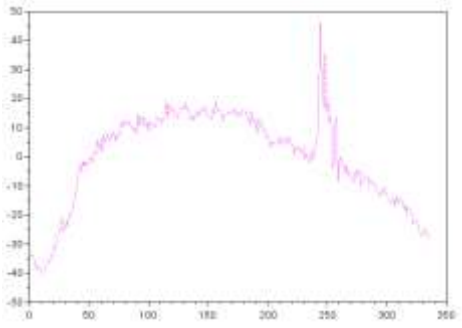

(a)

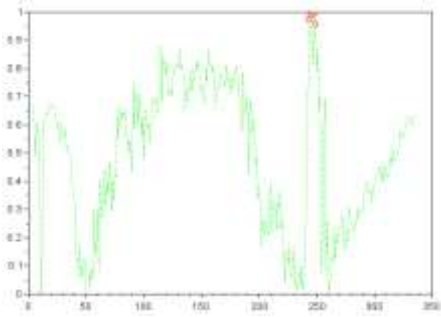

(b)

Fig. 8: Magnetic detection of MON100
a) after trend removal b) probability of detection

So, we can take optical detection confidence near 0.7, and magnetic detection probability near 0.97. From the formula, we will get:

$$p_{\Sigma} \cong \frac{0.7 \cdot 0.97}{0.7 \cdot 0.97 + (1-0.7) \cdot (1-0.97)} \cong 0.96$$

That is a rather satisfactory probability.

Antipersonnel landmine MON200 (Figure 9) is a more massive modification of MON100.

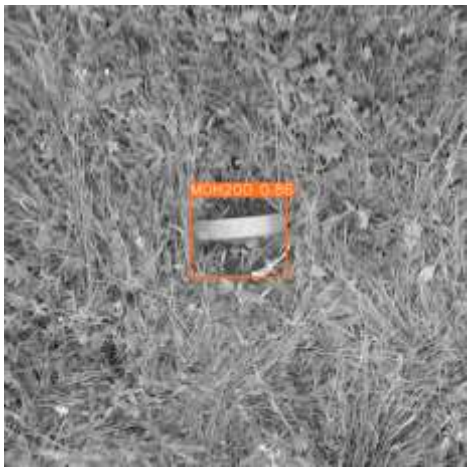

(a)

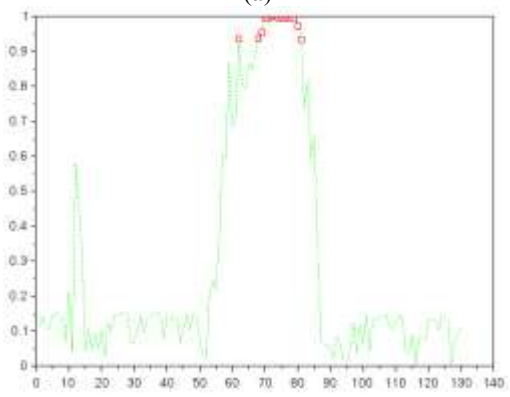

(b)

Fig. 9: Antipersonnel MON 200 detection: a) after trend removal and b) probability of detection

$$p_{\Sigma} \cong \frac{0.86 \cdot 0.97}{0.86 \cdot 0.97 + (1-0.86) \cdot (1-0.97)} \cong 0.995$$

One more antitank landmine of the TM series - TM72 (Figure 10).

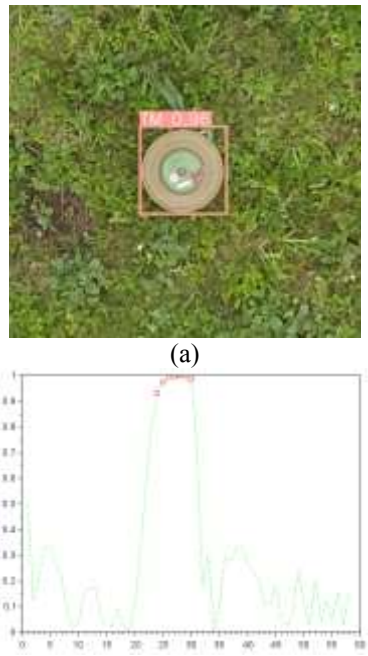

(a)

(b)

Fig. 10: Antitank TM72, a) optical detection and b) probability distribution acquired from magnetometer data:

$$p_{\Sigma} \cong \frac{0.96 \cdot 0.97}{0.96 \cdot 0.97 + (1-0.96) \cdot (1-0.97)} \cong 0.999$$

One more antipersonnel landmine MON90 (Figure 11).

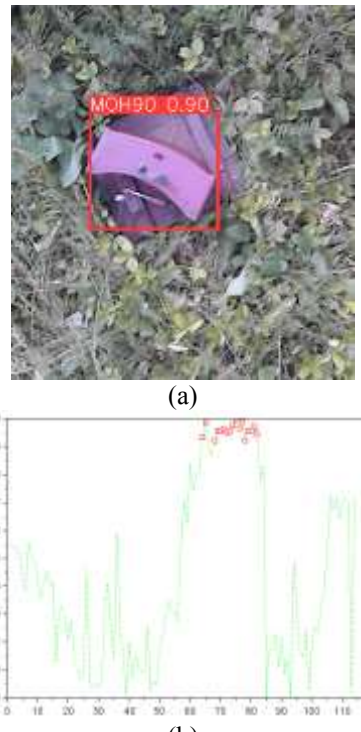

(a)

(b)

Fig. 11: Antipersonnel MON90:
a) optical detection, b) probability distribution from magnetometer data

$$p_{\Sigma} \cong \frac{0.90 \cdot 0.95}{0.9 \cdot 0.95 + (1-0.9) \cdot (1-0.95)} \cong 0.994$$

5 Discussion

In the approach demonstrated, an assumption was made that the confidence returned by CNN is of the same nature as the probability obtained by statistical anomaly detection done for magnetic detection. More theoretical explanation is needed to prove this concept or find an alternative way to calculate probability based on deep learning methods.

The two methods of detection chosen for demonstration are obviously at different levels of complexity and stages of development. Computer vision has rapidly advanced in recent years, significantly advancing methods of optical detection compared to those using magnetometers or ground-penetrating radar. There is potential for broader use of deep learning in magnetic detection. Further investigation is needed to prove the concept of not only detecting magnetic anomalies but also detecting magnetic signatures of different landmines. New tools are also required to simplify the preprocessing stage for magnetometric data.

6 Conclusion

As a result of the study, a general methodology of optical and magnetometric data integration for landmine detection with UAVs is proposed. This methodology ensures a unified probabilistic model for landmine detection using sensors of different physical natures, accompanied by the Bayesian summation of partial probabilities obtained. The output of the UAV-acquired data processing is a map of the landmine detection fused probability over the study area. The provided examples of landmine detection using optical and magnetometric data integration demonstrate an accuracy that is acceptable for practical applications.

The proposed methodology is flexible and universal, and it can be easily extended to other types of UAV onboard sensors, such as thermal infrared cameras or GPRs (ground penetrating radars).

Future research should be directed towards improving the recognition architecture, for example, using FSOD (few-shot object detection) [30], as well as refining the model for the integration of landmine detection outputs.

Acknowledgement:
The authors are grateful to the NAS of Ukraine for financial support, as well as to WSEAS for providing the opportunity for this publication.

References:

[1] Yang J., Xu R., Qi Z., Shi Y. Visual anomaly detection for images: a systematic survey, *Procedia Computer Science*, Vol.199, 2022, pp. 471-478, DOI: 10.1016/j.procs.2022.01.057.

[2] Popov M.O., Stankevich S.A., Mosov S.P., Titarenko O.V., Topolnytskyi M.V., Dugin S.S. Landmine detection with UAV-based optical data fusion, *Proceedings of the 19th International Conference on Smart Technologies* (EuroCon 2021, Lviv, Ukraine), IEEE, 2021, pp. 175-178, DOI: 10.1109/EUROCON52738.2021.9535553.

[3] Staszewski J.J., Davison A.D., Tischuk J.A., Dippel D.J. Visual cues for landmine detection, *Proceedings of SPIE, San Diego, California*, USA, Vol.6553, 2007, 65531H, DOI: 10.1117/12.723479

[4] Pimenta J.L.(2023, may 09) Identification of landmines in thermal infrared images, *Engineering Environmental Science*, 2015, [Online]. http://hdl.handle.net/10400.26/17894 (Accessed Date: October 3, 2024).

[5] Bajić M. Jr., Potočnik B. UAV thermal imaging for unexploded ordnance detection by using deep learning, *Remote Sensing*, Vol.15, No.4, 2023, 967, DOI: 10.3390/rs15040967.

[6] Barnawi A., Kumar K., Kumar N., Alzahrani B., Almansour A. A deep learning approach for landmines detection based on airborne magnetometry imaging and edge computing, *Computer Modeling in Engineering and Sciences*, Vol.139, No.2, 2024, pp. 2117-2137, DOI: 10.32604/cmes.2023.044184.

[7] Lee J., Lee H., Ko S., Ji D., Hyeon J. Modeling and implementation of a joint airborne ground penetrating radar and magnetometer system for landmine detection, *Remote Sensing*, Vol.15, No.15, 2023, 3813, DOI: 10.3390/rs15153813.

[8] Poliachenko I., Kozak V., Bakhmutov V., Cherkes S., & Varava I. Preliminary results of UAV magnetic surveys for unexploded ordnance detection in Ukraine: effectiveness and challenges, *Geophysical Journal*, Vol.45, No.5, 2023, pp. 126-140, DOI: 10.24028/gj.v45i5.289117.

[9] Ko K.H., Jang G., Park K., Kim K. GPR-based landmine detection and identification using multiple features, *International Journal of Antennas and Propagation*, Vol.2012, No.1, 2012, 826404, DOI: 10.1155/2012/826404.

[10] Maranhão P., Andraos L., Guedes R., Epprecht E. Landmine detection via multivariate image analysis, *The Journal of Defense Modeling and Simulation*, Vol.20, No.3, 2023, pp. 391-401, DOI: 10.1177/15485129221082048.

[11] Narkhede P., Walambe R., Kotecha K. Sensor Fusion Methodologies for Landmine Detection. In: Saraswat M., Chowdhury C., Mandal C.K., Gandomi A.H. (Eds.) *Lecture Notes in Networks and Systems*, Vol.551, Springer, 2023, pp. 891-907, DOI: 10.1007/978-981-19-6631-6_62.

[12] Popov M.O., Stankevich S.A., Mosov S.P., Titarenko O.V., Dugin S.S., Golubov S.I., Andreiev A.A. Method for minefields mapping by imagery from unmanned aerial vehicle, *Advances in Military Technology*, Vol.17, No.2, 2022, pp. 211-229, DOI: 10.3849/aimt.01722.

[13] Redmon J., Divvala S., Girshick R., Farhadi A. You Only Look Once: unified, real-time object detection. *Proceedings of the IEEE/CVF Conference on Computer Vision and Pattern Recognition (CVRP 2016). Las Vegas: IEEE, 2016*, pp., 779-788. DOI: 10.1109/CVPR.2016.91.

[14] Ultralytics (2024, June 12) Ultralytics YOLOv8 - State-of-the-art Vision AI, [Online]. https://www.ultralytics.com/yolo (Accessed Date: October 3, 2024).

[15] Baur, J., Steinberg, G., Nikulin, A., Chiu, K., Smet, T. (2020). Applying Deep Learning to Automate UAV-Based Detection of Scatterable Landmines. *Remote Sensing*. 12(5):859, DOI 10.3390/rs12050859.

[16] Cho S., Ma J., Yakimenko O.A. (2023) Aerial multi-spectral AI-based detection system for unexploded ordnance, *Defence Technology*, 27, 24-37, ISSN: 2214-9147, DOI: 10.1016/j.dt.2022.12.002.

[17] Qiu, Z.; Guo, H.; Hu, J.; Jiang, H.; Luo, C. (2023) Joint Fusion and Detection via Deep Learning in UAV-Borne Multispectral Sensing of Scatterable Landmine. *Sensors* 23(5693) DOI: 10.3390/s23125693.

[18] Diwan T., Anirudh G., Tembhurne J.V. Object detection using YOLO: challenges, architectural successors, datasets and applications. *Multimedia Tools and Applications*, 2023, vol. 82, no. 6, pp. 9243-9275. DOI: 10.1007/s11042-022-13644-y.

[19] Saprykin I. Optical deep learning landmine detection based on a limited dataset of aerial imagery, *Science-Based Technologies*, Vol.62, No.2, 2024, pp. 107-115, DOI: 10.18372/2310-5461.62.18708.

[20] Ram-Cohen T., Alimi R., Weiss E., Zalevsky Z. Characterization and detection of oscillating magnetic dipole signals, *Measurement Science and Technology*, Vol.28, No.4, 2017, 045104, DOI: 10.1088/1361-6501/aa59c0.

[21] Macharet D.G., Perez-Imaz H.I.A., Rezeck P.A.F., Potje G.A., Benyosef L.C.C., Wiermann A., Freitas G.M., Garcia L.G.U., Campos M.F.M. Autonomous aeromagnetic surveys using a fluxgate magnetometer, *Sensors*, Vol.16, No.12, 2016, 2169, DOI: 10.3390/s16122169.

[22] Gavazzi, B., P. Le Maire, M. Munschy, and A. Dechamp, 2016, Fluxgate vector magnetometers: A multisensor device for ground, UAV, and airborne magnetic surveys: *The Leading Edge*, 35, no. 9, 795–797, DOI: 10.1190/tle35090795.1.

[23] Munschy, M., D. Boulanger, P. Ulrich, and M. Bouiflane, 2007, Magnetic mapping for the detection and characterization of UXO: Use of multi-sensor fluxgate 3-axis magnetometers and methods of interpretation: *Journal of Applied Geophysics*, 61, nos. 3–4, 168–183, https://doi.org/10.1016/j.jappgeo.2006.06.004.

[24] Prouty, M. D., Tchernychev M., 2016, Real-time threat detection using magnetometer arrays: *Proceedings, Sensors, and Command, Control, Communications, and Intelligence (C3I) Technologies for Homeland Security, Defense, and Law Enforcement Applications, Baltimore, MD, United States* Volume 9825, XV, SPIE, https://doi.org/10.1117/12.2224338.

[25] Butler, D.K. (2003). Implications of magnetic backgrounds for unexploded ordnance detection. *Journal of Applied Geophysics, 54*(1-2), 111—25. https://doi.org/10.1016/j.jappgeo.2003.08.022.

[26] Nguyen T.T., Hao D.N., Lopez P., Cremer F., Sahli H. Thermal infrared identification of buried landmines. *Proceedings of SPIE*, San Diego, CA, United States, 2005, vol. 5794, pp. 198-208. DOI: 10.1117/12.626263.

[27] Lee J., Lee H. Modeling residual magnetic anomalies of landmines using UAV-borne vector magnetometer: flight simulations and experimental validation. *Remote Sensing*, 2024, vol. 16, no. 16, a. 2916. DOI: 10.3390/rs16162916.

[28] Zhang Y. The application of Bayesian theorem, *Highlights in Science, Engineering and Technology*, vol. 49, 2023, pp. 520-526, DOI: 10.54097/hset.v49i.8605.

[29] Rousseeuw P.J., Hubert M. Anomaly detection by robust statistics. *WIREs Data Mining and Knowledge Discovery*, 2018, vol. 8, no. 2, e1236. DOI: 10.1002/widm.1236.

[30] Han G., Lim S.-N. Few-shot object detection with foundation models. *Proceedings of the IEEE/CVF Conference on Computer Vision and Pattern Recognition (CVPR 2024). Seattle: IEEE*, 2024, pp. 28608-28618. DOI: 10.1109/CVPR52733.2024.02703.

Contribution of Individual Authors to the Creation of a Scientific Article (Ghostwriting Policy)

- Sergey A. Stankevich carried out conceptualization, methodology development, funding acquisition, and supervision.
- Ievgen Y. Saprykin was responsible for data curation, formal analysis, methodology development (partially), software development, visualization, and validation.

Sources of Funding for Research Presented in a Scientific Article or Scientific Article Itself

This research was supported by the NAS of Ukraine under the Target Scientific and Technical Program of Defense Research of the NAS of Ukraine for 2020-2024, contract No. НЦАД3-2024/1-1230

Conflict of Interest

The authors have no conflicts of interest to declare.